Sill-Controlled Circulation in Ice-Shelf Cavities

Ken X. Zhao, Andrew L. Stewart, and James C. McWilliams

Department of Atmospheric and Oceanic Sciences, UCLA

Contact Information

- Email: kzhao@atmos.ucla.edu
- Web: https://dept.atmos.ucla.edu/kenzhao/
- Addr: 9277 Boelter Hall, UCLA, Los Angeles

Research Overview

- Goal is to understand the sill-controlled transport and circulation regimes in an idealized ice-shelf cavity.
- Posed as 2-layer cavity circulation problem with imposed along-channel density gradient.
- Parameter regime is explored using numerical model, and phenomena are explained using PV balance and simplified uniform PV theory.

Pine Island Glacier (Motivation)

- Pine Island Glacier (PIG) is one of the most rapidly retreating glaciers.
- Bathymetric sill under Pine Island Glacier modulates inflow of warm Circumpolar Deep Water (CDW) into the ice-shelf cavity.[1,2,3]
- Warm, salty bottom layer inflows over sill and flows out above as (less dense) cold, fresh water after transformation near ice-shelf. This transformation occurs primarily close to the grounding line.

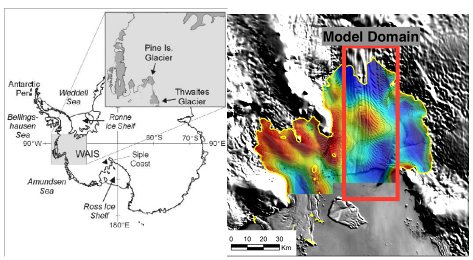

Figure 1: Pine Island Glacier location and geometry. Credit: Rignot et al. 2002 [1] and NASA [4].

Cavity Parameters

Cavity Size: W x L x H = 50km x 100km x 700m
Sill Height: H_{Sill} = 400 m
Density: ρ = 1027.47 - 1027.75 kg/m^3
Coriolis Parameter: $f = -1.41 \times 10^{-4} s^{-1}$
Transport: Q ~ 300 - 500 mSv
Internal Baroclinic Def. Radius: L_d = 5 km
Pressure Head: ΔH_2= 100 - 200 m
Drag Velocity: r = .1 - 14 $\times 10^{-5}$ m/s

Model Configuration

- Back of the Envelope Ocean Model (BEOM) is a hydrostatic shallow-water isopycnal model that simulates rotating basins with layer-outcropping.[5]
- We use a prescribed stratification nudging at north and south ends of channel instead of a fixed water mass transformation rate.

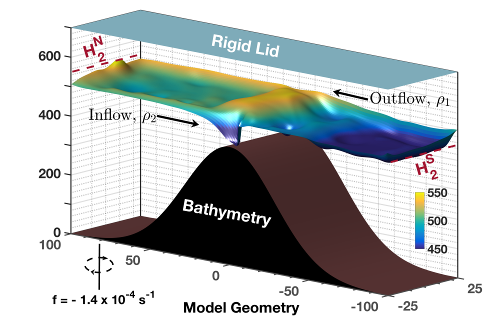

Figure 2: Representative geometry of low-drag, high-sill case (similar to PIG), with snapshot of η. Geostrophic boundary currents, variability, and a shock are evident.

Cross-Sill Exchange

- Sill height strongly controls the mean transport above critical threshold, drag primarily controls variability, and both drag and pressure head follow **geostrophic dynamics**

$$Q_{\text{geo}} \approx |f| L_d^2 \Delta H_2 . \quad (1)$$

- **Nondimensional parameters:**

Drag: $\hat{r} = r L_{\text{Sill}} H_2^N / (|f| L_d H_0 (H_2^N - H_0))$
Sill Height: $\widehat{H}_{\text{Sill}} = H_{\text{Sill}} / H_2^N$
Pressure Head: $\Delta \widehat{H}_2 = \Delta H_2 / H_2^N$ (2)

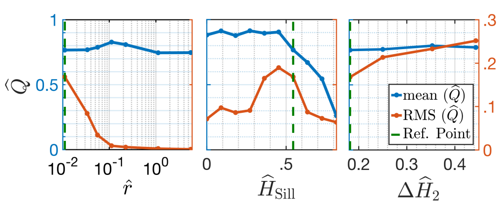

Figure 3: Mean and variance of transport $\hat{Q} = Q/Q_{\text{geo}}$ as a function of nondimensional drag, sill height, and pressure head.

High Drag Regime

- Steady solutions characterized by Stommel-balanced boundary currents, which cross sills gradually and symmetrically due to sign of β_{topo}.

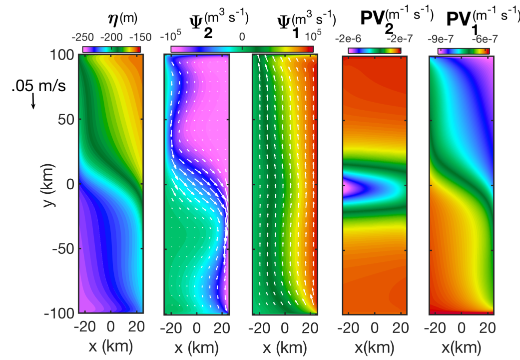

Figure 4: Numerical solution for the high-drag case showing interface displacement η and top and bottom transport streamfunction and PV.

Low Drag Regime

- Eddying solutions are observed, which depend on sill height. Unimpeded domain-filling circulation for low-sills, intensification of western boundary currents and eddies for intermediate sills, and emergence of shocks and abundant, small eddies for higher sills.

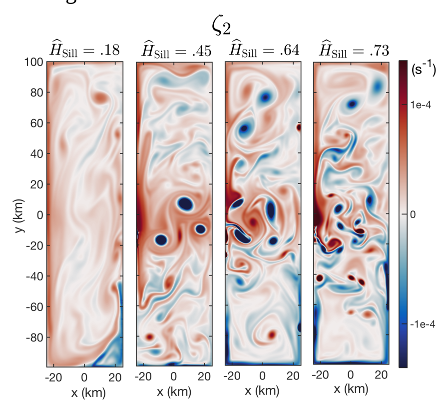

Figure 5: Snapshot of bottom layer vorticity ζ_2 for varying sill height for constant, low-drag cases.

Hydraulically-Controlled Regime

- Theoretical estimates for geostrophic and hydraulically-controlled transport match numerical results. Transport is geostrophic for low sills and decreases for controlled regime.

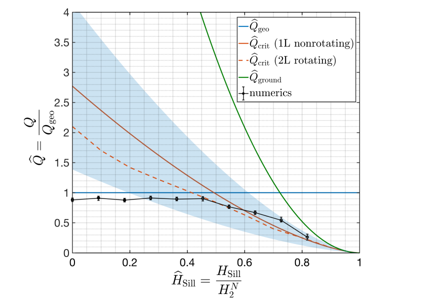

Figure 6: Predicted transport for geostrophic, critical, and grounded conditions and numerical results.

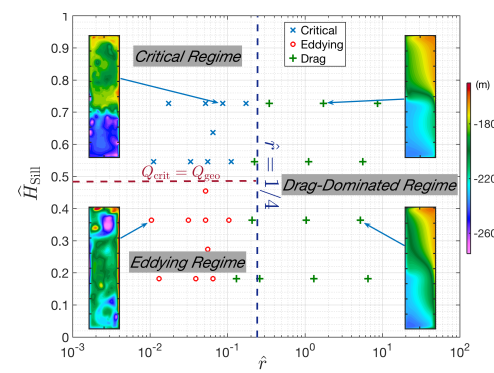

Figure 7: Regime diagram for nondimensional H_{Sill} vs. $\hat{r}$.

Summary and Future Work

- 3 parameter regimes described in 2-layer cavity flows depending on **sill height** and **drag**.
- Transport set by along-channel thermal shear for low sills and hydraulic control for high sills. Variability controlled by drag.
- Further work will include responsive diabatic forcing in the cavity (i.e. realistic ice melt and consequent buoyancy forcing) and study the response of an evolving ice-shelf.

References: [1] Rignot, E., Vaughan, D.G., Schmeltz, M., Dupont, T., MacAyeal, D. (2002) Acceleration of Pine Island and Thwaites Glaciers, West Antarctica. Annals of Glaciology, 34, 189-194. [2] Jenkins, A., Dutrieux, P., Jacobs, S., McPhail, S.D., Perrett, J. R., Webb, A.T., White, D. (2010) Observations beneath Pine Island Glacier in West Antarctica and implications for its retreat. Nature Geoscience, 3, 468-472. [3] De Rydt, J., Holland, P.R., Dutrieux, P., Jenkins, A. (2014) Geometric and oceanographic controls on melting beneath Pine Island Glacier. J. Geophys. Res. Oceans, 119, 2420–2438. [4] NASA. Operation IceBridge campaign bathymetry data, 2009. Retrieved from: www.nasa.gov/mission pages/icebridge/ [5] St-Laurent, Pierre. Back of the Envelope Ocean Model (BEOM). Source code available under copyleft license: http://www.nordet.net/beom.html